

# General relativistic simulations of the quasi-circular inspiral and merger of charged black holes: GW150914 and fundamental physics implications

Gabriele Bozzola<sup>1,\*</sup> and Vasileios Paschalidis<sup>2,†</sup>

<sup>1</sup>*Department of Astronomy, University of Arizona, Tucson, AZ, USA*

<sup>2</sup>*Departments of Astronomy and Physics, University of Arizona, Tucson, AZ, USA*

(Dated: January 28, 2021)

We perform general-relativistic simulations of charged black holes targeting GW150914. We show that the inspiral is most efficient for detecting black hole charge through gravitational waves and that GW150914 is compatible with having charge-to-mass ratio as high as 0.3. Our work applies to electric and magnetic charge, and to theories with black holes endowed with U(1) (hidden or dark) charges. Using our results we place an upper bound on the deviation from general relativity in the dynamical, strong-field regime of the so-called theory of MODified Gravity (MOG).

**Introduction** According to the “no-hair” conjecture [1–6], general relativistic black holes are described by four parameters: mass, angular momentum, electric and magnetic charge. It is assumed, often implicitly, that astrophysical black holes have negligible charge because of the expectation that they would quickly discharge due to the interaction with a highly conducting gaseous environment or by the spontaneous production of electron-positron pairs [7–12]. However, observational data unequivocally supporting this expectation are currently absent, and any existing constraints on black hole charge depend crucially on the assumptions of the models employed (e.g. [13, 14]). Gravitational-wave observations offer a model-independent path to constraining the charge of astrophysical black holes. The electromagnetic fields influence the spacetime, altering the gravitational-wave emission compared to an uncharged binary. These deviations are accurately modeled in Einstein-Maxwell theory, and are potentially detectable by LIGO-Virgo and future gravitational-wave observatories. As we will discuss below, the word “charge” here is an umbrella term that includes, among other things, electric or magnetic charge, dark charge, or gravitational charge due to modifications to general relativity.

In this letter, we initiate a robust program for constraining black hole charge by combining LIGO-Virgo observations with novel numerical relativity simulations. Our focus here is on event GW150914 [15].<sup>1</sup> Using the event’s sky location and the calibrated LIGO noise, we compute the *mismatch* (defined later) between the uncharged case and various charged ones. The observed signal-to-noise ratio sets a threshold mismatch above which two waveforms are distinguishable [25–28]. Hence, assuming that the observed waveform is described by uncharged, non-spinning black holes, we find the minimum charge that would be detectable by LIGO.

For uncharged binaries, when black hole spin is ne-

glected and the mass-ratio is fixed, knowing one “mass” parameter determines the entire gravitational waveform. We will use here the *chirp mass*  $\mathcal{M}$  [29]. In the case of inspirals of charged binaries, this parameter can be degenerate with the charge itself [30–33]. This can be understood as follows: In Newtonian physics, gravity and electromagnetism are both central potentials, so the electrostatic force can be accounted for by introducing an effective Newton constant  $\tilde{G}$ . Consider two bodies with mass  $m_1, m_2$  and charge  $q_1 = \lambda_1 m_1, q_2 = \lambda_2 m_2$  ( $\lambda$  being the charge-to-mass ratio); the dynamics of the system is indistinguishable from one with uncharged bodies with gravitational constant  $\tilde{G} = (1 - \lambda_1 \lambda_2)G$ . Since the relationship between chirp mass and gravitational-wave frequency evolution involves Newton’s constant, introducing charges corresponds to rescaling the chirp mass while keeping  $G$  fixed. This degeneracy is broken by electromagnetic radiation reaction and the field self-gravity.

Adopting the effective Newton constant approach, previous studies [30–35] constructed Newtonian-based waveforms by considering the Keplerian motion of two charged bodies and accounting for loss of energy via quadrupolar emission of gravitational waves and dipolar emission of electromagnetic ones. The authors of [31] computed the bias in the binary parameters due to the charge-chirp mass degeneracy. With similar tools, [35] performed a full Bayesian analysis with Gaussian noise to place preliminary constraints on charge using events in the first gravitational wave transient catalog [36]. Alternatively, the dipole can be constrained directly by adding a  $-1\text{PN}$  (Post-Newtonian) term to describe the loss of energy due to dipole emission [35], as first done for modified theories of gravity [37]. In [37, 38], it was found that the dipole can be constrained more effectively in the inspiral (also noted in [30, 33] with explicit reference to charges). One of the main limitations of these (post)-Newtonian methods is that they strictly apply only to the early inspiral. However, binaries like GW150914 are in the regime where numerical relativity simulations are necessary for accurate modeling [15]. Therefore, existing constraints on black hole charge in events where only a few orbits

<sup>1</sup> The possibility that GW150914 involved charged black holes has been invoked [16–18] to explain the observation of a coincident electromagnetic signal by Fermi-GBM [19, 20]. This association is debated as others satellites did not detect the event [21–24].

to merger have been detected are at best preliminary. Moreover, the effective Newton constant approach does not capture the physics in cases when only one of the two components is charged, and when the dipole moment vanishes these previous approaches do not treat quadrupole electromagnetic emission. This is very important because as we demonstrate here, it is binaries with near vanishing dipole moment that place the weakest constraint on black hole charge.

A second avenue for constraining black hole charge is through the ringdown signal. In the context of mergers of charged black holes, this was first studied in [30, 33] in the limit of small charge, using the method of geodesic correspondence. Via a Fisher matrix analysis, it was noticed that the ability to constrain charge depends strongly on the signal-to-noise ratio, so GW150914 cannot be used to place strong bounds on the charge-to-mass ratio  $\lambda$  of the final black hole. However, as the authors remarked, these results should be considered only as qualitative, since higher-order terms in  $\lambda$  were neglected.

Instead of using approximations, here we solve the full non-linear Einstein-Maxwell equations, extracting accurate gravitational waves to overcome the shortcomings of previous approaches. We perform numerical-relativity simulations of black holes with (1) same charge-to-mass ratio (that we will indicate with  $\lambda_+^+$ ) (2) same charge-to-mass ratio but opposite sign ( $\lambda_-^+$ ), and (3) only one charged black hole ( $\lambda_0^+$ ). Einstein-Maxwell theory has no intrinsic scale, so our simulations scale with the total ADM (Arnowitt-Deser-Misner) mass of the system  $M$  [39]. Thus, we can explore arbitrary chirp masses with each simulation. We compute the mismatch between gravitational waveforms generated by charged and uncharged binaries with a range of different masses to account for the degeneracy: black hole charge is constrained when the mismatch is larger than a value set by the signal-to-noise ratio [25–28] for all possible values of the chirp mass.

An important advantage of our approach is that it furnishes a first-principles calculation based on fundamental theories, and does not rely on particular models. As a result, the mathematical formulation we employ has direct fundamental physics applications. Examples are dark matter theories (e.g., *dark electromagnetism*, *hidden sector* [31, 40–45], or *mini-charged* particles [30, 46–53]). These theories allow black holes to be highly charged, since neutralization arguments do not apply. Moreover, with a duality transformation [54], our work also constrains black hole magnetic charge (e.g., from primordial magnetic monopoles [55, 56]). Our simulations are also useful for the generation and calibration of gravitational-wave template banks that target these systems.

Furthermore, our research targets theories of gravitation where gravity is also mediated by a vector field, like the scalar-tensor-vector gravity developed in [57] to explain “dark matter” phenomenology without dark mat-

ter. This theory (also known with the acronym “MOG” – Modified Gravity), has been widely studied in the past and can pass several tests, such as Solar System ones [58] (see also [57, 59–67]; for a summary of the formulation, assumptions, and successes of the theory, see [62]). MOG features a scalar field that makes gravity stronger by increasing Newton’s constant and a Proca field that counteracts this effect in the short range. When considering systems much smaller than the galactic scale, the vector field can be considered massless and the scalar field becomes constant and modifies Newton’s constant to  $G_{\text{eff}} = G(1 + \alpha)$ . According to MOG, a body with mass  $M$  has a *gravitational charge*  $Q$  that is associated with the vector field and is proportional to  $M$ . *Moffat’s prescription* sets the constant of proportionality to  $\sqrt{\alpha G_{\text{eff}}/(1 + \alpha)}$  so that the theory satisfies the weak equivalence principle [68]. In this limit, MOG differs mathematically from Einstein-Maxwell theory only in using  $G_{\text{eff}}$  instead of  $G$ , and when  $\alpha = 0$  the theory becomes general relativity. This rescaling gives rise to the same degeneracy in the chirp mass and  $\tilde{G}$  that we discussed above in the case of electromagnetism: in geometrized units, MOG solutions with mass  $M_{\text{MOG}}$  and gravitational constant  $G_{\text{eff}} = 1$  are equivalent to Einstein-Maxwell solutions with mass  $M = M_{\text{MOG}}(1 + \alpha)$  and  $G = 1$ . Hence, by scanning through all possible values of the mass, a constraint on the charge-to-mass ratio translates in this theory to a constraint on  $Q/M = \sqrt{\alpha/(1 + \alpha)}$ .

The results of this work depend on three assumptions: 1) Einstein-Maxwell theory is the correct description of charged black holes at the energy, length, and time scales we are investigating; 2) GW150914 is accurately modeled by waveforms from uncharged, non-spinning binary black holes with mass ratio 29/36—the value inferred for GW150914 [15]; 3) The black hole spin and binary mass ratio remain that of GW150914 even in the case of non-zero charge. Spin and mass ratio may be degenerate with the charge, so the results presented in this paper can be interpreted in two ways: if assumption 3) holds for GW150914, then our charge limits are *upper bounds* on the charge-to-mass ratio of the binary components, otherwise, they are lower bounds on the charge-to-mass ratio needed to leave detectable imprints in GW150914-like events. We will explore the effects of spin and mass ratio in future works. To further reduce the parameter space, we only consider black holes with the same charge-to-mass ratio bracketing the possibilities. This choice also ensures the applicability of our results to modified theories of gravity where the charge-to-mass-ratio represents a coupling constant (as in MOG), in which case only systems with the same charge-to-mass-ratio are relevant (in the limit we discussed above).

**Methods** We employ the *Einstein Toolkit* [69–72] to solve the coupled Einstein-Maxwell equations in the  $3 + 1$  decomposition of four-dimensional spacetime [39, 73–76]. We report the general features of our approach

here and leave the details for the Supplemental Material.

We performed simulations with charge-to-mass ratio  $\lambda \in \{0.01, 0.05, 0.1, 0.2, 0.3\}$  with like or opposite charge for the two black holes (cases that we will designate as  $\lambda_+^+$  and  $\lambda_-^+$ , where the superscript and subscript indicate the sign of the charge of the primary and the secondary, respectively), and only one charged black hole ( $\lambda_0^+$ ). These cases are supplemented by an uncharged one ( $\lambda_0^0$ ), a convergence study, and by simulations with  $\lambda_+^+ = 0.4$ ,  $\lambda_0^+ = 0.35$ , and  $\lambda_+^0 = 0.35$ .

Full non-linear evolutions of Einstein-Maxwell systems have already been performed in the past for head-on collisions of charged black holes [77, 78]. Simulations of quasi-circular inspirals are a non-trivial extension of that as the generation of valid initial data with the solution of the constraint equations [75] is required. In [79] we presented `TwoChargedPunctures`, which solves this problem by adopting an extended Bowen-York formalism [80–82] and allows the generation of arbitrary configurations of charged black holes. We fix the initial coordinate separation to  $12.1 M$  and we choose the black hole initial linear momenta to yield a quasi-circular inspiral using a 2.5PN estimate after rescaling  $G$  to  $\tilde{G}$ .

We evolve the spacetime and electromagnetic fields with the open-source and well-tested `Lean` and `ProcaEvolve` codes [83–86]. `Lean` implements the Baumgarte-Shapiro-Shibata-Nakamura formulation of Einstein’s equation [87, 88], while `ProcaEvolve` evolves the electromagnetic vector potential with a constraint-damping scheme for the Gauss constraint. The evolution is on Cartesian `Carpet` [89] grids where the highest resolution is approximately  $M/65$ , with  $M$  being the binary ADM mass [39]. We extract gravitational waves based on the Newman-Penrose formalism [86, 90], adopting the fixed-frequency integration method [91]. We decompose the signal into  $-2$  spin weighted spherical harmonics, and focus on the dominant  $l = 2$ ,  $m = 2$  gravitational wave mode.

Two waveforms are considered experimentally indistinguishable if their mismatch is smaller than  $1/(2\rho^2)$  [25–28], with  $\rho$  being the signal-to-noise ratio. For GW150914,  $\rho = 25.1$  [92], so the threshold mismatch above which two signals are distinguishable is approximately  $8 \times 10^{-4}$ . We calculate the mismatch between strains  $h_1$  and  $h_2$  as  $1 - \max \mathcal{O}(h_1, h_2)$ , where  $\mathcal{O}(h_1, h_2)$  is the overlap between the two signals (see Supplemental Material), and the maximum is evaluated with respect to time-shifts, orbital-phase shifts and polarization angles [28, 93]. The overlap calculation is performed in the frequency domain. We consider LIGO’s noise curve at the time of GW150914 detection, and adopt the GW150914 inferred sky location. For the uncharged signal, we set a source frame ADM mass  $M = 65 M_\odot$ , and a luminosity distance of 410 Mpc, corresponding to cosmological redshift of  $\approx 0.09$  [94]. In the Supplemental Material we discuss how different choices for these parameters

affect the results. To account for the charge-chirp mass degeneracy, we compute the mismatch between gravitational waves from uncharged black holes and the ones from charged systems with different chirp masses  $\mathcal{M}$ . To vary the chirp mass, we rescale  $M$  by a factor that we indicate with  $\mathcal{M}/\mathcal{M}_{00}$ , where  $\mathcal{M}_{00}$  is the chirp mass of the uncharged simulation. We estimate the error on the mismatch by comparing simulations at different resolutions.

**Results and Discussion** The mismatch between a charged and the uncharged binary grows with the charge-to-mass ratio  $\lambda$ . So, we may place an upper bound on the charge by finding the value of  $\lambda$  at which the minimum mismatch (as we vary the chirp mass) is larger than  $8 \times 10^{-4}$ . We find that, assuming negligible spin and mass ratio of 29/36, GW150914 constrains  $\lambda$  to be smaller than

$$\lambda_+^+ = 0.4, \quad \lambda_-^+ = 0.2, \quad \text{and} \quad \lambda_0^+ = 0.35. \quad (1)$$

Regardless of the value of the spin and the mass ratio, Equation (1) provide lower bounds on  $\lambda$  needed to have detectable effects in GW150914-like events.

In our simulations we always endow the more massive black hole with positive charge. Since the mass asymmetry of the system is small, we expect our conclusions to remain the same in the opposite case. The simulation with  $\lambda_+^0 = 0.35$  confirms this expectation: the computed minimum mismatch differs by 10% from the  $\lambda_0^+ = 0.35$  case. Thus, the effect of the mass asymmetry is small.

In Figure 1, we show the mismatch between the uncharged simulation and charged ones as a function of the rescaling factor  $\mathcal{M}/\mathcal{M}_{00}$  for the chirp mass. The figure has three sets of curves. Solid curves represent the mismatch computed on the entirety of the signal (i.e., all frequencies are included). In the top panels, these curves have minima below the threshold mismatch (horizontal solid line) for some value of  $\mathcal{M}/\mathcal{M}_{00}|_{\min}$ . Thus, gravitational waves from these charged configurations are indistinguishable from the signal that we adopt as true for GW150914. The opposite holds in the bottom panels. Therefore, under the assumptions of our study, GW150914 is compatible with involving charged black holes with  $Q/M$  up to about 0.3. The noise curve adopted plays an important role: if instead of the realistic one, we consider the Zero-Detuned-High-Power noise curve [95], the mismatch increases by a factor of about 3, making the top panels in Figure 1 incompatible with the observation, and hence distinguishable. Thus, it is important to use the realistic noise in these calculations.

Figure 1 reports two additional sets of curves: dashed lines, representing the mismatch computed including frequencies below 55 Hz, and dotted ones for frequencies above 55 Hz. In other words, the dashed and dotted curves are the mismatch that would be computed if we had detected *only* the inspiral or *only* the plunge and

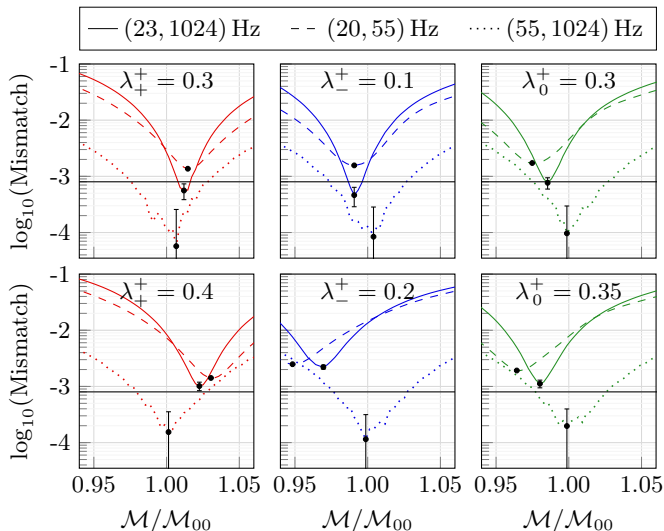


FIG. 1. Mismatch between the strains from uncharged black holes and from charged ones with chirp mass rescaled by  $\mathcal{M}/\mathcal{M}_{00}$ . Solid curves are the mismatch including all available frequencies (the entire signal), dashed ones are only restricting to the frequency range (23, 55) Hz (inspiral) and dotted ones have frequencies restricted to (55, 1024) Hz (merger and ringdown). The solid horizontal line is the detection threshold for GW150914 ( $8 \times 10^{-4}$ ). The top (bottom) row is the largest (smallest) value of  $\lambda$  (in our survey) compatible (incompatible) with GW150914. Red curves (left panels) are for the simulation with  $\lambda_+^+ = 0.3$  (top) and  $\lambda_+^+ = 0.4$  (bottom), blue (central panels) for  $\lambda_+^+ = 0.1$  and  $\lambda_+^+ = 0.2$ , and green (middle panels) for  $\lambda_0^+ = 0.3$  and  $\lambda_0^+ = 0.35$ . The error bars shown are estimated comparing the standard resolution simulation with the one at higher resolution. We report the error bar only at minimum mismatch, but each point along the curve has the same level of error.

merger phases. The frequency of 55 Hz marks conventionally the end of the *inspiral* phase [96]. Including a larger range of frequencies, decreases the minimum mismatch (from dashed lines to solid). Hence, previous studies focusing only on the inspiral overestimate the mismatch and the bias in the extracted chirp mass.

Figure 1 shows that the mismatch is significantly higher in the inspiral, suggesting that it is the dominant contribution in the overall mismatch. Figure 2 further emphasizes this conclusion: we plot the strain the Hanford detector would observe, if there was no noise, i.e.,  $h_{\text{Hanford}}^{22} = F_{\times} h_{\times}^{22} + F_{+} h_{+}^{22}$ , where  $F$  is the detector antenna pattern [92]. The dashed curves represent GW150914 and the solid ones are the strains from the charged simulations, rescaled and shifted to maximize the overlap. The plot shows that the greatest difference between charged and uncharged black holes arises in the earlier inspiral. Thus, signals that stay for a longer duration in LIGO-Virgo bands allow for stronger constraints on the charge. All waveforms in Figure 2 have mismatch with GW150914 larger than  $8 \times 10^{-4}$ , hence

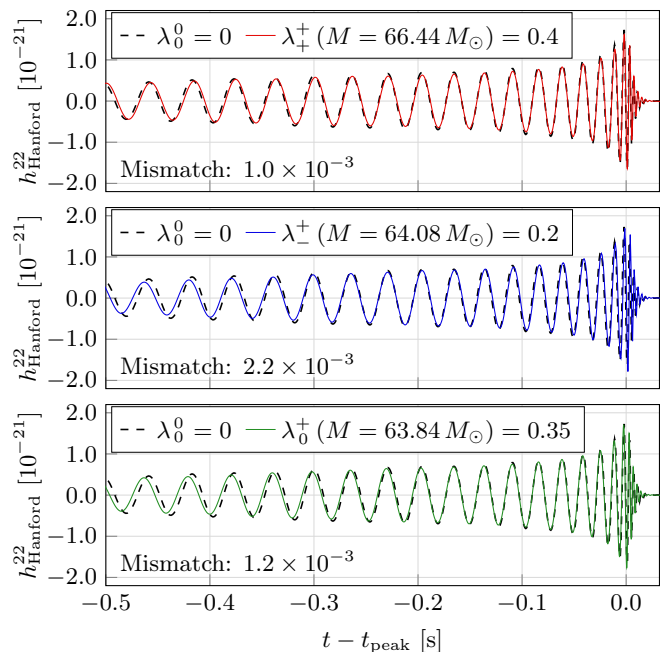


FIG. 2. Comparison between the (2, 2) mode of the detector-response strain for Hanford for the simulations with no charges (dashed curves) and the ones with it, but with chirp mass  $\mathcal{M}$  rescaled with respect to  $\mathcal{M}_{00} = 28.095 M_{\odot}$ . Time and phase shifts are applied to minimize the mismatch between the two signals. All of these waveforms have two-detectors mismatch larger than the detection threshold for GW150914 of  $8 \times 10^{-4}$ , mostly coming from the inspiral phase.

the corresponding charge configurations are incompatible with GW150914.

One of the reasons why the merger+ringdown phase of the signal is not as informative as the inspiral is that the properties of the final black holes do not depend strongly on the initial charge configuration. In all our simulations, the mass of the final black hole is the same to within 1% ( $M_{\text{final}} \approx 0.96 M$ ), and the dimensionless spin differs by at most 6% ( $a_{\text{final}}/M_{\text{final}} \approx 0.66$ ). In particular, in our opposite charge cases, the final mass and spin have sub-percent differences with respect to the uncharged case, and, as expected from relativistic estimates, the case with same charge has a lower spin [97]. This result agrees with [30, 33]: a large charge or a large signal-to-noise ratio is required to extract the charge information from the ringdown.

Our full non-linear study supports previous results that were obtained with parametrized methods. Constraints on the dipolar gravitational-wave emission were placed in [37, 38] using Fisher matrix analysis based on phenomenological waveform models. Translated into an upper bound on the normalized electric dipole, the constraint becomes  $\zeta = |\lambda_1 - \lambda_2|/\sqrt{1 - \lambda_1 \lambda_2} \lesssim 0.31$  [30, 35]. Our work shows that  $\zeta < 0.3$  (from the case

with  $\lambda_0^+ = 0.3$ ). However, our work goes further by placing a constraint on the individual black hole charge.

Our results can also be applied to the so-called theory of MOdified Gravity (MOG) [98]. At scales relevant for compact binary mergers, this theory replaces Newton's constant  $G \rightarrow G_{\text{eff}}$ , and postulates the existence of a *gravitational charge*  $Q = \sqrt{\alpha G_{\text{eff}}/(1 + \alpha)}M$ . The difference in Newton's constant is degenerate with a change in chirp mass, which we thoroughly explored. Figure 1 shows that when  $\lambda_{\pm}^+ = 0.4$  no matter how the chirp mass is changed, it is not possible to reconcile GW150914 with the merger of charged black holes with  $\lambda_{\pm}^+ = 0.4$ . Hence, our study directly constrains  $\alpha \lesssim 0.19$ . This implies that the theory cannot deviate much from general relativity in the strong field, under the assumptions made in this work.

**Conclusions** In this letter, we presented fully self-consistent general relativistic simulations of the inspiral and merger of charged non-spinning black holes with mass ratio 29/36. We considered cases where both black holes are charged with the same charge-to-mass ratio ( $\lambda_{\pm}^+$ ), opposite charge-to-mass ratio ( $\lambda_{\pm}^-$ ), and only one black hole charged ( $\lambda_0^+$ ). By comparing waveforms from uncharged systems to those from charged ones, we addressed the charge-chirp mass degeneracy and found that, assuming non-spinning black holes with mass ratio of 29/36 for GW150914,  $\lambda$  has to be smaller than:

$$\lambda_{\pm}^+ = 0.4, \quad \lambda_{\pm}^- = 0.2, \quad \text{and} \quad \lambda_0^+ = 0.35. \quad (2)$$

These results hold under the assumption that spin and mass-ratio play a secondary role. Independently of that, Equation (2) provides a lower bound on the charge-to-mass ratio needed to leave measurable effects on the gravitational waves from GW150914-like events.

We found that the inspiral is the most constraining part of the signal for charge (Figures 1, 2). So, low-mass binaries, having more orbits in LIGO-Virgo bands, will likely yield tighter bounds on black hole charge. Our full non-linear analysis confirms that it is challenging to constrain charge from the ringdown phase of merging charged black holes [30, 33].

The bounds found in this study do not apply only to electric charge, but they can be directly translated to constraints on modified theories of gravity and exotic astrophysical scenarios, e.g., dark matter models [30], or primordial magnetic monopoles [55]. In this work, we applied our findings to Moffat's scalar-vector-tensor gravity (SVTG or MOG) [57] and constrained its  $\alpha$  parameter to  $\alpha \lesssim 0.19$  (note that  $\alpha = 0$  is general relativity). Here, we did not consider the effects of black hole spin and the binary mass ratio and including these parameters can introduce degeneracies that make the constraint less stringent. Applications to lower-mass black hole binary detections may be able to constrain this theory significantly in the strong field, dynamical regime.

In the future, we will consider systems with spinning black holes, different mass-ratios, and asymmetric charge-to-mass ratio. With a large enough bank of simulations, we will produce surrogate models (e.g. [99]) to perform full parameter estimation of GW150914 and other LIGO-Virgo events.

*Acknowledgments* We thank M. Zilhão for help on **ProcaEvolve**, J. R. Westernacher-Schneider for useful discussions, and D. Brown, V. Cardoso, J. Moffat and U. Sperhake for comments on the manuscript. We also wish to thank D. Brown for discussions on gravitational-wave data analysis. We are grateful to the developers and maintainers of the open-source codes that we used: their work was essential to the research presented here. This work was in part supported by NSF Grant PHY-1912619 to the University of Arizona. We acknowledge the hospitality of the Kavli Institute for Theoretical Physics (KITP), where part of the work was conducted. KITP is partially supported by the NSF grant No. PHY-1748958. Computational resources were provided by the Extreme Science and Engineering Discovery Environment (XSEDE) under grant number TG-PHY190020. XSEDE is supported by the NSF grant No. ACI-1548562. Simulations were performed on **Comet**, and **Stampede2**, which is funded by the NSF through award ACI-1540931.

### Supplemental material

**Details of the numerical methods** We generate constraint-satisfying initial data with **TwoChargedPunctures**, which can build arbitrary configurations of charged binary black holes. The values of the initial black hole linear momenta are chosen to yield a quasi-circular inspiral. To do so, we first use a 2.5 post-Newtonian expression to determine the values required to generate a quasi-circular inspiral in the uncharged case. Next, for given charge-to-mass ratios  $\lambda_1$  and  $\lambda_2$ , we rescale  $G$  to  $\bar{G}$ , by multiplying the linear momenta with  $\sqrt{1 - \lambda_1 \lambda_2}$  (since they are proportional to  $\sqrt{G}$ ). For the initial orbital separation chosen, and the charge-to-mass ratios explored, this choice yields near quasi-circular inspirals: estimating the eccentricity with the method described in [100] or in the Appendix of [101], the maximum eccentricity after the first orbit is 0.005, except in the  $\lambda_{\pm}^+ = 0.3$  case, where it is 0.014. Our experiments show that our method for setting the initial black hole linear momenta must be modified to achieve very low eccentricity in simulations with black holes that have close to extremal and opposite charges (i.e., large  $\lambda_{\pm}^+$ ), in which case eccentricity-reduction methods or more sophisticated post-Newtonian expansions that include the electromagnetic fields may be required.

For the time integration of the Einstein-Maxwell equations we use the method of lines with a fourth-order Runge-Kutta scheme. The spacetime evolution is performed adopting sixth-order finite-differences

with the `Lean` code [85], which is based on the Baumgarte-Shapiro-Shibata-Nakamura (BSSN) formulation [87, 88] of the Einstein equations, and exploits the puncture approach for the black-hole singularities. Apparent horizons are located with `AHFinderDirect` [102, 103], and their physical properties [104, 105] are computed with `QuasiLocalMeasuresEM`—a version of `QuasiLocalMeasures` [106] we extended to implement the formalism of quasi-isolated horizons in full Einstein-Maxwell theory [79]. Maxwell’s equations are evolved also using sixth-order finite differences with the `ProcaEvolve` code [86], which is designed to keep the magnetic and electric fields divergenceless. We adopt the Lorenz gauge for the electromagnetic sector, and the  $1+\log$  and  $\Gamma$ -freezing gauge conditions for the lapse function and shift vector [107–109]. To improve the stability of the simulation, we add seventh-order Kreiss-Oliger dissipation [110] to all evolved variables and we introduce an extra parabolic term to the equations for the evolution of the electric field to further dissipate violations of Gauss’s constraint. The choice of the dissipation parameters is critical to ensure long-term evolutions, in particular, high dissipation is needed near the black holes, and but stability near the outer boundary requires lower Kreiss-Oliger dissipation. We will present the details in an upcoming paper that will provide an in-depth discussion on the formalism. Both `Lean` and `ProcaEvolve` are part of the `Canuda` open-source suite [83] and have already been tested and used in previous studies (e.g. [85, 86]).

We employ `Carpet` [89] for moving-box adaptive mesh-refinement, and use nine refinement levels. The outer boundary is placed at  $1033 M$  where we impose outgoing-wave boundary conditions. We performed selected simulations with outer boundary twice as far, and found that all reported quantities are invariant with the outer boundary location to within one part in  $10^8$ . Sixth-order accurate evolutions with such grid configurations are computationally expensive. Most of our simulations were performed on ten nodes on the `Stampede2` (480 Skylake Intel CPUs, 1.92 TB of volatile memory and comparable storage) and took up to several weeks of wall time to be completed. Evolutions for different  $\lambda$  were run concurrently and, as expected, the cases with black holes charged with the same sign required significantly more time.

The extraction of gravitational and electromagnetic waves is performed at ten different spatial radii in the range ( $45.19 M, 192.74 M$ ). In this work we report quantities at the extraction radius  $111.69 M$ . We checked that our results do not depend on the extraction radius, and small differences from different radii are taken into account in our error budget. We remove the first period from the extracted signals as it contains *junk* radiation from the initial data [111, 112].

We calculate the mismatch between strains  $h_1$  and  $h_2$

as [28, 93]

$$\text{mismatch}(h_1, h_2) = 1 - \max \mathcal{O}(h_1, h_2), \quad (3)$$

with the maximum evaluated with respect to time-shifts, orbital-phase shifts and polarization angles. Here,  $\mathcal{O}(h_1, h_2)$  is the overlap between  $h_1$  and  $h_2$

$$\mathcal{O}(h_1, h_2) = \frac{(h_1, h_2)}{\sqrt{(h_1, h_1)(h_2, h_2)}} \quad (4)$$

with  $(h_1, h_2)$  being the two-detector noise-weighted inner product between the two signals in the frequency domain  $\tilde{h}_1(f)$  and  $\tilde{h}_2(f)$ , [113]

$$(h_1, h_2) = \sum_{\substack{\text{Hanford} \\ \text{Livingston}}} \left[ 4 \text{Re} \int_{f_{\min}}^{f_{\max}} \frac{\tilde{h}_1(f) \tilde{h}_2^*(f)}{S_n(f)} df \right], \quad (5)$$

where  $S_n(f)$  is the power spectral noise, and an asterisk denotes complex conjugation. We crop the waveforms to ensure that they all end at the same time after merger. Then we apply a Tukey window to the time series with parameter 0.1 so that the signal goes smoothly to zero. We pad numerical waveforms with zeros so that all frequency series have the same length, and we take discrete Fourier transforms. We consider three choices for the combination  $(f_{\min}, f_{\max})$ : (23, 1024) Hz to include the entire signal; (23, 55) Hz to take into account only the “inspiral” (at least six orbits) and (55, 1024) Hz for the plunge and post-merger phases (corresponding to approximately the last two cycles). We choose these frequencies following the LIGO-Virgo collaboration in identifying the first part as *inspiral*, and the second is what LIGO-Virgo further splits in *intermediate + merger and ringdown* [96]. This second group of frequencies is in the most sensitive range for LIGO. The lowest frequency in our simulations is approximately 23 Hz. For  $S_n(f)$ , we employ the calibrated noise registered in coincidence with GW150914 (downloaded from the Gravitational Waves Open Science Center [114]). We use the inferred sky location of the source (right ascension: 8 h, declination:  $-70^\circ$ , UTC time: 09:50:45.39 September 14 2015) and the corresponding gravitational-wave antenna pattern of the two detectors [92].

**Error budget and convergence** Our simulations exhibit excellent conservation of total energy, total angular momentum, and total charge. Summing up the mass of the final black hole, and the energies carried away by gravitational and electromagnetic waves, we find the initial ADM energy to within 1 part in  $2 \times 10^4$ . Similarly, angular momentum is conserved to within 1 part in  $7 \times 10^3$ . In these calculations we also extrapolate waves to spatial infinity following [109] and include all harmonic modes up to  $l = 8$ . Results are nearly invariant if a finite extraction radius is considered instead. For energy and angular momentum radiated we use the

Newman-Penrose scalars [115, 116]. Charge is conserved to a high degree of accuracy: if  $Q_1, Q_2$  are the initial horizon charges and  $Q_{\text{final}}$  the final black hole charge computed by `QuasiLocalMeasuresEM` [79], we find that  $|Q_{\text{final}} - (Q_1 + Q_2)| / (|Q_1| + |Q_2|) \leq 2 \times 10^{-5}$ .

For the case  $\lambda_{\pm}^{\pm} = 0.3$  we performed a convergence study by considering resolutions 25% higher ( $M/81$ ) and lower ( $M/52$ ) compared to the canonical one. Among our cases,  $\lambda_{\pm}^{\pm} = 0.3$  exhibits the highest velocities, and strongest emission of energy and angular momentum in gravitational and electromagnetic waves. The high-resolution simulation is also used to provide an estimate for the error of the standard resolution simulations. The conserved quantities reported in the previous paragraph improve by a factor of  $\approx 2$  for the simulation at higher resolution.

We show convergence more formally in Figure 3, where we report the absolute value of the difference of  $h_{+}^{22}$  between different resolutions (and similarly for  $h_{\times}^{22}$ ). Early on we observe the well-known resolution-dependent high-frequency noise [117, 118] due to reflection/diffraction phenomena across refinement-level boundaries. After an initial noise-dominated phase, the difference between the two higher resolution simulations (orange dashed curve) becomes smaller than the one between the two lower-resolution runs (blue solid line), demonstrating self-convergence.

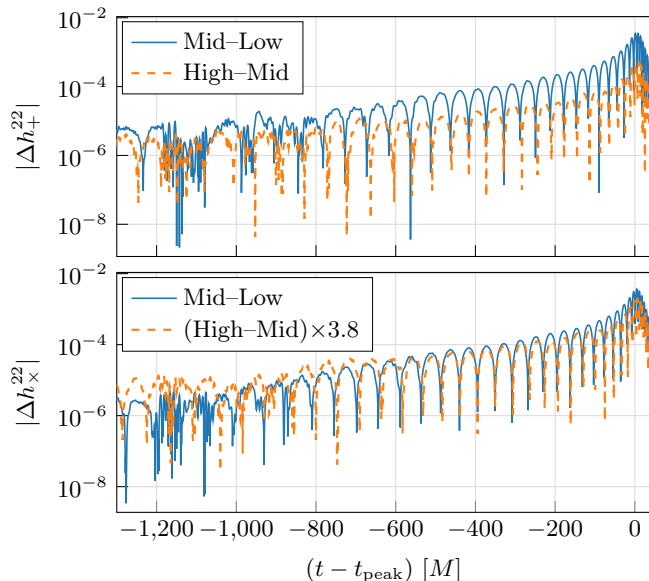


FIG. 3. Self-convergence of the plus and cross polarization of the strain for simulations with  $\lambda_{\pm}^{\pm} = 0.3$ . The blue solid (orange dashed) lines are the absolute value of the difference between the strain at medium and low (high and medium) resolution. In the bottom panel we rescale the difference between the high and medium resolutions assuming sixth order convergence, i.e., by a factor of  $(1.25)^6 \approx 3.8$ , where 1.25 is the ratio between the resolutions.

We estimate the error of the mismatch by finding the maximum mismatch between the simulation with standard resolution and the one with higher resolution with respect to changing the extraction radius, the cutoff frequency for the fixed-frequency integration, and the amount of signal cropped at the beginning of the simulation to remove “junk” radiation. We find an error of  $1.5 \times 10^{-4}$  for the total signal,  $3 \times 10^{-5}$  for frequencies up to 55 Hz, and  $2 \times 10^{-4}$  for frequencies above 55 Hz. These numbers are well below the LIGO GW150914 threshold mismatch of  $8 \times 10^{-4}$  for distinguishing two different waveforms. The minimum of the mismatch when only considering high frequencies alone is of the same order as our error, which explains why the dotted curves in Figure 1 are noisier compared to the other ones. This systematic error in our simulation prevents us from estimating what signal-to-noise ratio would be needed to extract charge information from the ringdown phase (see dotted lines in Figure 1).

To confirm that the mismatch we compute is due to the presence of charge and not the residual initial eccentricity, we use `EccentricFD` [119]—a non-spinning frequency-domain, inspiral-only template available in `PyCBC` [120, 121]. Focusing on the inspiral (up to 55 Hz), we find that the values of eccentricity we measure in our simulations ( $\approx 0.005$ ) produce mismatches that are at least one order of magnitude smaller than the ones we reported in the main text. Even for the largest eccentricity we measure (0.014), the computed mismatch remains subdominant ( $\approx 2 \times 10^{-4}$ ). Therefore, this assures us that for the large values of  $\lambda$  in our survey, the mismatch is due to black hole charge and not to the initial eccentricity.

**Confidence levels** In the main text, we represent GW150914 as an uncharged binary black hole with total mass  $65 M_{\odot}$ , at a luminosity distance of 410 Mpc, and use for the signal-to-noise ratio  $\rho$  the value 25.1. These are the most probable parameters for the event according to the Bayesian analysis performed by the LIGO-Virgo collaboration [92]. Moreover, we adopted as threshold mismatch for distinguishing two signals the standard choice of  $1/(2\rho^2)$ . Using Equation (18) in [122] (with one degree of freedom  $k = 1$  since we compare charged configurations with an uncharged one, and maximize the overlap over all other parameters), a mismatch of  $1/(2\rho^2)$  corresponds to a 68% confidence level. The most probable parameters represent neither the worst nor the best case scenario for distinguishing black hole charge. The worst-case-scenario is when both the number of gravitational wave cycles in LIGO’s sensitivity band and the signal-to-noise ratio are minimized: for GW150914 this happens when the distance is 570 Mpc and the total mass is  $69.5 M_{\odot}$ , which are the largest values in LIGO’s 90% confidence levels. The minimum signal-to-noise ratio reported by LIGO is  $\rho = 23.4$ . Even under these conditions, our constraint on  $\lambda_{\pm}^{\pm}$  remains unchanged, but for

the  $\lambda_+^+ = 0.4$  case, the threshold mismatch for distinguishing charge must reduce to  $6.8 \times 10^{-4}$ , making the confidence level of our constraint (based on Equation (18) in [122]) 61 %.

---

\* gabrielebozzola@arizona.edu

† vpaschal@arizona.edu

- [1] W. Israel, Event Horizons in Static Vacuum Space-Times, *Physical Review* **164**, 1776 (1967).
- [2] B. Carter, Axisymmetric Black Hole Has Only Two Degrees of Freedom, *Physical Review Letters* **26**, 331 (1971).
- [3] D. C. Robinson, Classification of black holes with electromagnetic fields, *Phys. Rev. D* **10**, 458 (1974).
- [4] S. W. Hawking, Black holes in general relativity, *Communications in Mathematical Physics* **25**, 152 (1972).
- [5] R. Hansen, Multipole moments of stationary space-times, *J. Math. Phys.* **15**, 46 (1974).
- [6] P. T. Chruściel, J. L. Costa, and M. Heusler, Stationary Black Holes: Uniqueness and Beyond, *Living Reviews in Relativity* **15**, 7 (2012), arXiv:1205.6112 [gr-qc].
- [7] R. M. Wald, Black hole in a uniform magnetic field, *Phys. Rev. D* **10**, 1680 (1974).
- [8] G. W. Gibbons, Vacuum polarization and the spontaneous loss of charge by black holes, *Communications in Mathematical Physics* **44**, 245 (1975).
- [9] D. M. Eardley and W. H. Press, Astrophysical processes near black holes, *Ann. Rev. Astron. Astrophys.* **13**, 381 (1975).
- [10] R. S. Hanni, Limits on the charge of a collapsed object, *Phys. Rev. D* **25**, 2509 (1982).
- [11] Y. Gong, Z. Cao, H. Gao, and B. Zhang, On neutralization of charged black holes, *Mon. Not. R. Astron. Soc.* **488**, 2722 (2019), arXiv:1907.05239 [gr-qc].
- [12] Z. Pan and H. Yang, Black hole discharge: Very-high-energy gamma rays from black hole-neutron star mergers, *Phys. Rev. D* **100**, 043025 (2019), arXiv:1905.04775 [astro-ph.HE].
- [13] L. Iorio, Constraining the electric charges of some astronomical bodies in Reissner-Nordström spacetimes and generic  $r^{-2}$ -type power-law potentials from orbital motions, *General Relativity and Gravitation* **44**, 1753 (2012), arXiv:1112.3520 [gr-qc].
- [14] M. Zajaček, A. Tursunov, A. Eckart, and S. Britzen, On the charge of the Galactic centre black hole, *Mon. Not. R. Astron. Soc.* **480**, 4408 (2018), arXiv:1808.07327.
- [15] B. P. Abbott *et al.* (LIGO Scientific Collaboration and Virgo Collaboration), Observation of gravitational waves from a binary black hole merger, *Phys. Rev. Lett.* **116**, 061102 (2016), 1602.03837.
- [16] B. Zhang, Mergers of Charged Black Holes: Gravitational-wave Events, Short Gamma-Ray Bursts, and Fast Radio Bursts, *Astrophys. J. Lett.* **827**, L31 (2016), arXiv:1602.04542 [astro-ph.HE].
- [17] S. L. Liebling and C. Palenzuela, Electromagnetic luminosity of the coalescence of charged black hole binaries, *Phys. Rev. D* **94**, 064046 (2016), arXiv:1607.02140 [gr-qc].
- [18] F. Fraschetti, Possible role of magnetic reconnection in the electromagnetic counterpart of binary black hole merger, *Journ. Cosm. Astrop. Phys.* **4**, 054 (2018), arXiv:1603.01950 [astro-ph.HE].
- [19] V. Connaughton, E. Burns, A. Goldstein, L. Blackburn, M. S. Briggs, B.-B. Zhang, J. Camp, N. Christensen, C. M. Hui, P. Jenke, T. Littenberg, J. E. McEnery, J. Racusin, P. Shawhan, L. Singer, J. Veitch, C. A. Wilson-Hodge, P. N. Bhat, E. Bissaldi, W. Cleveland, G. Fitzpatrick, M. M. Giles, M. H. Gibby, A. von Kienlin, R. M. Kippen, S. McBreen, B. Mailyan, C. A. Meegan, W. S. Paciesas, R. D. Preece, O. J. Roberts, L. Sparke, M. Stanbro, K. Toelge, and P. Veres, Fermi GBM Observations of LIGO Gravitational-wave Event GW150914, *Astrophys. J. Lett.* **826**, L6 (2016), arXiv:1602.03920 [astro-ph.HE].
- [20] V. Connaughton, E. Burns, A. Goldstein, L. Blackburn, M. S. Briggs, N. Christensen, C. M. Hui, D. Kocevski, T. Littenberg, J. E. McEnery, J. Racusin, P. Shawhan, J. Veitch, C. A. Wilson-Hodge, P. N. Bhat, E. Bissaldi, W. Cleveland, M. M. Giles, M. H. Gibby, A. von Kienlin, R. M. Kippen, S. McBreen, C. A. Meegan, W. S. Paciesas, R. D. Preece, O. J. Roberts, M. Stanbro, and P. Veres, On the Interpretation of the Fermi-GBM Transient Observed in Coincidence with LIGO Gravitational-wave Event GW150914, *Astrophys. J. Lett.* **853**, L9 (2018), arXiv:1801.02305 [astro-ph.HE].
- [21] B. P. Abbott, R. Abbott, T. D. Abbott, M. R. Abernathy, F. Acernese, K. Ackley, C. Adams, T. Adams, P. Addesso, R. X. Adhikari, and et al., Localization and Broadband Follow-up of the Gravitational-wave Transient GW150914, *Astrophys. J. Lett.* **826**, L13 (2016), arXiv:1602.08492 [astro-ph.HE].
- [22] K. Hurley, D. S. Svinikin, R. L. Aptekar, S. V. Golenetskii, D. D. Frederiks, W. Boynton, I. G. Mitrofanov, D. V. Golovin, A. S. Kozyrev, M. L. Litvak, A. B. Sanin, A. Rau, A. von Kienlin, X. Zhang, V. Connaughton, C. Meegan, T. Cline, and N. Gehrels, The Interplanetary Network Response to LIGO GW150914, *Astrophys. J. Lett.* **829**, L12 (2016).
- [23] P. A. Evans, J. A. Kennea, S. D. Barthelmy, A. P. Beardmore, D. N. Burrows, S. Campana, S. B. Cenko, N. Gehrels, P. Giommi, C. Gronwall, F. E. Marshall, D. Malesani, C. B. Markwardt, B. Mingo, J. A. Nousek, P. T. O'Brien, J. P. Osborne, C. Pagani, K. L. Page, D. M. Palmer, M. Perri, J. L. Racusin, M. H. Siegel, B. Sbarufatti, and G. Tagliaferri, Swift follow-up of the gravitational wave source GW150914, *Mon. Not. R. Astron. Soc.* **460**, L40 (2016), arXiv:1602.03868 [astro-ph.HE].
- [24] V. Savchenko, C. Ferrigno, S. Mereghetti, L. Natalucci, A. Bazzano, E. Bozzo, S. Brandt, T. J.-L. Courvoisier, R. Diehl, L. Hanlon, A. von Kienlin, E. Kuulkers, P. Laurent, F. Lebrun, J. P. Roques, P. Ubertini, and G. Weidenspointner, INTEGRAL Upper Limits on Gamma-Ray Emission Associated with the Gravitational Wave Event GW150914, *Astrophys. J. Lett.* **820**, L36 (2016), arXiv:1602.04180 [astro-ph.HE].
- [25] É. É. Flanagan and S. A. Hughes, Measuring gravitational waves from binary black hole coalescences. II. The waves' information and its extraction, with and without templates, *Phys. Rev. D* **57**, 4566 (1998), gr-qc/9710129.
- [26] L. Lindblom, B. J. Owen, and D. A. Brown, Model waveform accuracy standards for gravitational wave data analysis, *Phys. Rev. D* **78**, 124020 (2008), arXiv:0809.3844 [gr-qc].
- [27] S. T. McWilliams, B. J. Kelly, and J. G. Baker, Observing mergers of nonspinning black-hole binaries, *Phys. Rev. D* **82**, 024014 (2010), arXiv:1004.0961 [gr-qc].
- [28] B. P. Abbott, R. Abbott, T. D. Abbott, M. R. Abernathy, F. Acernese, K. Ackley, C. Adams, T. Adams, P. Addesso, R. X. Adhikari, and et al., Effects of waveform model systematics on the interpretation of GW150914, *Classical and Quantum Gravity* **34**, 104002 (2017), arXiv:1611.07531 [gr-qc].
- [29] M. Maggiore, *Gravitational Waves. Vol. 1: Theory and Experiments*, Oxford Master Series in Physics (Oxford University Press, 2007).
- [30] V. Cardoso, C. F. B. Macedo, P. Pani, and V. Ferrari, Black holes and gravitational waves in models of minicharged dark matter, *J. Cosm. Astropart. Phys.* **5**, 054 (2016), arXiv:1604.07845 [hep-ph].
- [31] Ø. Christiansen, J. Beltrán Jiménez, and D. F. Mota, Charged Black Hole Mergers: Orbit Circularisation and Chirp Mass Bias, arXiv e-prints, arXiv:2003.11452 (2020), arXiv:2003.11452 [gr-qc].

- [32] L. Liu, Z.-K. Guo, R.-G. Cai, and S. P. Kim, Merger rate distribution of primordial black hole binaries with electric charges, arXiv e-prints , arXiv:2001.02984 (2020), [arXiv:2001.02984 \[astro-ph.CO\]](#).
- [33] V. Cardoso, C. F. B. Macedo, P. Pani, and V. Ferrari, Erratum: Black holes and gravitational waves in models of minicharged dark matter Erratum: Black holes and gravitational waves in models of minicharged dark matter, *J. Cosm. Astropart. Phys.* **2020**, E01 (2020).
- [34] L. Liu, Ø. Christiansen, Z.-K. Guo, R.-G. Cai, and S. P. Kim, Gravitational and electromagnetic radiation from binary black holes with electric and magnetic charges: Circular orbits on a cone, *Phys. Rev. D* **102**, 103520 (2020), [arXiv:2008.02326 \[gr-qc\]](#).
- [35] H.-T. Wang, P.-C. Li, J.-L. Jiang, Y.-M. Hu, and Y.-Z. Fan, Post-Newtonian waveform for charged binary black hole inspirals and analysis with GWTC-1 events, arXiv e-prints , arXiv:2004.12421 (2020), [arXiv:2004.12421 \[gr-qc\]](#).
- [36] B. P. Abbott, R. Abbott, T. D. Abbott, S. Abraham, F. Acernese, K. Ackley, C. Adams, R. X. Adhikari, V. B. Adya, C. Affeldt, and et al., GWTC-1: A Gravitational-Wave Transient Catalog of Compact Binary Mergers Observed by LIGO and Virgo during the First and Second Observing Runs, *Physical Review X* **9**, 031040 (2019), [arXiv:1811.12907 \[astro-ph.HE\]](#).
- [37] E. Barausse, N. Yunes, and K. Chamberlain, Theory-Agnostic Constraints on Black-Hole Dipole Radiation with Multiband Gravitational-Wave Astrophysics, *Phys. Rev. Lett.* **116**, 241104 (2016), [arXiv:1603.04075 \[gr-qc\]](#).
- [38] N. Yunes, K. Yagi, and F. Pretorius, Theoretical physics implications of the binary black-hole mergers GW150914 and GW151226, *Phys. Rev. D* **94**, 084002 (2016), [arXiv:1603.08955 \[gr-qc\]](#).
- [39] R. L. Arnowitt, S. Deser, and C. W. Misner, The dynamics of general relativity, *General Relativity and Gravitation* **40**, 1997 (2008), [arXiv:gr-qc/0405109](#).
- [40] J. L. Feng, M. Kaplinghat, H. Tu, and H.-B. Yu, Hidden charged dark matter, *J. Cosm. Astropart. Phys.* **2009**, 004 (2009), [arXiv:0905.3039 \[hep-ph\]](#).
- [41] L. Ackerman, M. R. Buckley, S. M. Carroll, and M. Kamionkowski, Dark matter and dark radiation, *Phys. Rev. D* **79**, 023519 (2009), [arXiv:0810.5126 \[hep-ph\]](#).
- [42] R. Foot and S. Vagnozzi, Dissipative hidden sector dark matter, *Phys. Rev. D* **91**, 023512 (2015), [arXiv:1409.7174 \[hep-ph\]](#).
- [43] R. Foot and S. Vagnozzi, Diurnal modulation signal from dissipative hidden sector dark matter, *Physics Letters B* **748**, 61 (2015), [arXiv:1412.0762 \[hep-ph\]](#).
- [44] R. Foot and S. Vagnozzi, Solving the small-scale structure puzzles with dissipative dark matter, *J. Cosm. Astropart. Phys.* **2016**, 013 (2016), [arXiv:1602.02467 \[astro-ph.CO\]](#).
- [45] P. Agrawal, F.-Y. Cyr-Racine, L. Randall, and J. Scholtz, Make Dark Matter Charged Again, *JCAP* **05**, 022, [arXiv:1610.04611 \[hep-ph\]](#).
- [46] S. Davidson, B. Campbell, and D. Bailey, Limits on particles of small electric charge, *Phys. Rev. D* **43**, 2314 (1991).
- [47] M. L. Perl and E. R. Lee, The search for elementary particles with fractional electric charge and the philosophy of speculative experiments, *American Journal of Physics* **65**, 698 (1997).
- [48] S. Davidson, S. Hannestad, and G. Raffelt, Updated bounds on milli-charged particles, *Journal of High Energy Physics* **5**, 003 (2000), [hep-ph/0001179](#).
- [49] S. L. Dubovsky, D. S. Gorbunov, and G. I. Rubtsov, Narrowing the window for millicharged particles by CMB anisotropy, *Soviet Journal of Experimental and Theoretical Physics Letters* **79**, 1 (2004), [arXiv:hep-ph/0311189 \[astro-ph\]](#).
- [50] A. D. Dolgov, S. L. Dubovsky, G. I. Rubtsov, and I. I. Tkachev, Constraints on millicharged particles from Planck data, *Phys. Rev. D* **88**, 117701 (2013), [arXiv:1310.2376 \[hep-ph\]](#).
- [51] H. Vogel and J. Redondo, Dark radiation constraints on minicharged particles in models with a hidden photon, *J. Cosm. Astropart. Phys.* **2014**, 029 (2014), [arXiv:1311.2600 \[hep-ph\]](#).
- [52] P. Gautham A. and S. Sethi, Cosmological implications of electromagnetically interacting dark matter: milli-charged particles and atoms with singly and doubly charged dark matter, *J. Cosm. Astropart. Phys.* **2020**, 039 (2020), [arXiv:1910.04779 \[astro-ph.CO\]](#).
- [53] R. Plestid, V. Takhistov, Y.-D. Tsai, T. Bringmann, A. Kusenko, and M. Pospelov, New Constraints on Millicharged Particles from Cosmic-ray Production, arXiv e-prints , arXiv:2002.11732 (2020), [arXiv:2002.11732 \[hep-ph\]](#).
- [54] J. D. Jackson, *Classical electrodynamics* (Wiley, 1975).
- [55] J. Preskill, Magnetic Monopoles, *Annual Review of Nuclear and Particle Science* **34**, 461 (1984).
- [56] D. Stojkovic and K. Freese, A black hole solution to the cosmological monopole problem, *Physics Letters B* **606**, 251 (2005), [hep-ph/0403248](#).
- [57] J. W. Moffat, Scalar-tensor-vector gravity theory, *Journal of Cosmology and Astroparticle Physics*. **2006**, 004 (2006).
- [58] J. W. Moffat, Scalar and Vector Field Constraints, Deflection of Light and Lensing in Modified Gravity (MOG), arXiv e-prints , arXiv:1410.2464 (2014), [arXiv:1410.2464 \[gr-qc\]](#).
- [59] J. R. Brownstein and J. W. Moffat, Galaxy Rotation Curves without Nonbaryonic Dark Matter, *Astrophys. J.* **636**, 721 (2006), [arXiv:astro-ph/0506370 \[astro-ph\]](#).
- [60] J. R. Brownstein and J. W. Moffat, Galaxy cluster masses without non-baryonic dark matter, *Mon. Not. R. Astron. Soc.* **367**, 527 (2006), [arXiv:astro-ph/0507222 \[astro-ph\]](#).
- [61] F. G. Lopez Armengol and G. E. Romero, Scalar-Tensor-Vector Gravity: solutions with matter content, *Boletín de la Asociación Argentina de Astronomía La Plata Argentina* **58**, 231 (2016).
- [62] F. G. Lopez Armengol and G. E. Romero, Neutron stars in Scalar-Tensor-Vector Gravity, *General Relativity and Gravitation* **49**, 27 (2017), [arXiv:1611.05721 \[gr-qc\]](#).
- [63] F. G. Lopez Armengol and G. E. Romero, Effects of Scalar-Tensor-Vector Gravity on relativistic jets, *Astrophys. Spac. Sci.* **362**, 214 (2017), [arXiv:1611.09918 \[astro-ph.HE\]](#).
- [64] F. Shojai, S. Cheraghchi, and H. Bouzari Nezhad, On the gravitational instability in the Newtonian limit of MOG, *Physics Letters B* **770**, 43 (2017), [arXiv:1704.04161 \[gr-qc\]](#).
- [65] D. Pérez, F. G. L. Armengol, and G. E. Romero, Accretion disks around black holes in scalar-tensor-vector gravity, *Phys. Rev. D* **95**, 104047 (2017), [arXiv:1705.02713 \[astro-ph.HE\]](#).
- [66] N. Ghafourian and M. Roshan, Global stability of self-gravitating discs in modified gravity, *Mon. Not. R. Astron. Soc.* **468**, 4450 (2017).
- [67] M. A. Green, J. W. Moffat, and V. T. Toth, Modified gravity (MOG), the speed of gravitational radiation and the event GW170817/GRB170817A, *Physics Letters B* **780**, 300 (2018), [arXiv:1710.11177 \[gr-qc\]](#).
- [68] J. W. Moffat, LIGO GW150914 and GW151226 gravitational wave detection and generalized gravitation theory (MOG), *Physics Letters B* **763**, 427 (2016), [arXiv:1603.05225 \[gr-qc\]](#).
- [69] F. Löffler, J. Faber, E. Bentivegna, T. Bode, P. Diener, R. Haas, I. Hinder, B. C. Mundim, C. D. Ott, E. Schnetter, G. Allen, M. Campanelli, and P. Laguna, The Einstein Toolkit: A Community Computational Infrastructure for Relativistic Astrophysics, *Class. Quantum Grav.* **29**, 115001 (2012), [arXiv:1111.3344 \[gr-qc\]](#).
- [70] Collaborative Effort, Einstein Toolkit for Relativistic Astrophysics, *Astrophysics Source Code Library* (2011), [ascl:1102.014](#).
- [71] Einstein Toolkit, *Einstein Toolkit: Open software for relativistic astrophysics* (2019).
- [72] M. Babiuc-Hamilton, S. R. Brandt, P. Diener, M. Elley, Z. Etienne, G. Ficarra, R. Haas, H. Witek, M. Alcubierre,

- D. Alic, G. Allen, M. Ansorg, L. Baiotti, W. Bengert, E. Bentivegna, S. Bernuzzi, T. Bode, B. Bruegmann, G. Corvino, R. D. Pietri, H. Dimmelmeier, R. Dooley, N. Dorband, Y. E. Khamra, J. Faber, T. Font, J. Friebe, B. Giacomazzo, T. Goodale, C. Gundlach, I. Hawke, S. Hawley, I. Hinder, S. Husa, S. Iyer, T. Kellermann, A. Knapp, M. Koppitz, G. Lanferman, F. Löffler, J. Masso, L. Menger, A. Merzky, M. Miller, P. Moesta, P. Montero, B. Mundim, A. Nerozzi, C. Ott, R. Paruchuri, D. Pollney, D. Radice, T. Radke, C. Reisswig, L. Rezzolla, D. Rideout, M. Ripeanu, E. Schnetter, B. Schutz, E. Seidel, E. Seidel, J. Shalf, U. Sperhake, N. Stergioulas, W.-M. Suen, B. Szilagyi, R. Takahashi, M. Thomas, J. Thornburg, M. Tobias, A. Tonita, P. Walker, M.-B. Wan, B. Wardell, M. Zilhão, B. Zink, and Y. Zlochower, *The einstein toolkit* (2019), to find out more, visit <http://einstein toolkit.org>.
- [73] K. S. Thorne and D. MacDonald, Electrodynamics in Curved Spacetime - 3+1 Formulation, *Mon. Not. R. Astron. Soc.* **198**, 339 (1982).
- [74] M. Alcubierre, *Introduction to 3+1 Numerical Relativity* (Oxford University Press, UK, 2008).
- [75] T. W. Baumgarte and S. L. Shapiro, *Numerical Relativity: Solving Einstein's Equations on the Computer* (Cambridge University Press, 2010).
- [76] M. Shibata, *Numerical Relativity* (World Scientific Publishing Co, 2016).
- [77] M. Zilhão, V. Cardoso, C. Herdeiro, L. Lehner, and U. Sperhake, Collisions of charged black holes, *Phys. Rev. D* **85**, 124062 (2012), [arXiv:1205.1063 \[gr-qc\]](https://arxiv.org/abs/1205.1063).
- [78] M. Zilhão, V. Cardoso, C. Herdeiro, L. Lehner, and U. Sperhake, Collisions of oppositely charged black holes, *Phys. Rev. D* **89**, 044008 (2014), [arXiv:1311.6483 \[gr-qc\]](https://arxiv.org/abs/1311.6483).
- [79] G. Bozzola and V. Paschalidis, Initial data for general relativistic simulations of multiple electrically charged black holes with linear and angular momenta, *Phys. Rev. D* **99**, 104044 (2019), [arXiv:1903.01036 \[gr-qc\]](https://arxiv.org/abs/1903.01036).
- [80] J. M. Bowen and J. York, James W., Time asymmetric initial data for black holes and black hole collisions, *Phys. Rev. D* **21**, 2047 (1980).
- [81] J. M. Bowen, Inversion symmetric initial data for N charged black holes., *Annals of Physics* **165**, 17 (1985).
- [82] M. Alcubierre, J. C. Degollado, and M. Salgado, Einstein-Maxwell system in 3+1 form and initial data for multiple charged black holes, *Phys. Rev. D* **80**, 104022 (2009), [arXiv:0907.1151 \[gr-qc\]](https://arxiv.org/abs/0907.1151).
- [83] H. Witek and M. Zilhão, *Canuda code* (2015), <https://bitbucket.org/canuda/>.
- [84] H. Witek, M. Zilhao, G. Ficarra, and M. Elley, *Canuda: a public numerical relativity library to probe fundamental physics* (2020).
- [85] U. Sperhake, Binary black-hole evolutions of excision and puncture data, *Phys. Rev. D* **76**, 104015 (2007), [gr-qc/0606079](https://arxiv.org/abs/gr-qc/0606079).
- [86] M. Zilhão, H. Witek, and V. Cardoso, Nonlinear interactions between black holes and Proca fields, *Classical Quant. Grav.* **32**, 234003 (2015), [arXiv:1505.00797 \[gr-qc\]](https://arxiv.org/abs/1505.00797).
- [87] M. Shibata and T. Nakamura, Evolution of three-dimensional gravitational waves: Harmonic slicing case, *Phys. Rev. D* **52**, 5428 (1995).
- [88] T. W. Baumgarte and S. L. Shapiro, Numerical integration of einstein's field equations, *Phys. Rev. D* **59**, 024007 (1998).
- [89] E. Schnetter, S. H. Hawley, and I. Hawke, Evolutions in 3-D numerical relativity using fixed mesh refinement, *Class. Quantum Grav.* **21**, 1465 (2004), [arXiv:gr-qc/0310042](https://arxiv.org/abs/gr-qc/0310042).
- [90] E. Newman and R. Penrose, An Approach to Gravitational Radiation by a Method of Spin Coefficients, *Journal of Mathematical Physics* **3**, 566 (1962).
- [91] C. Reisswig and D. Pollney, Notes on the integration of numerical relativity waveforms, *Classical Quant. Grav.* **28**, 195015 (2011), [arXiv:1006.1632 \[gr-qc\]](https://arxiv.org/abs/1006.1632).
- [92] B. P. Abbott, R. Abbott, T. D. Abbott, M. R. Abernathy, F. Acernese, K. Ackley, C. Adams, T. Adams, P. Addesso, R. X. Adhikari, and et al., Properties of the Binary Black Hole Merger GW150914, *Physical Review Letters* **116**, 241102 (2016), [arXiv:1602.03840 \[gr-qc\]](https://arxiv.org/abs/1602.03840).
- [93] T. Damour, B. R. Iyer, and B. S. Sathyaprakash, Improved filters for gravitational waves from inspiraling compact binaries, *Phys. Rev. D* **57**, 885 (1998), [gr-qc/9708034](https://arxiv.org/abs/gr-qc/9708034).
- [94] Planck Collaboration, N. Aghanim, Y. Akrami, M. Ashdown, J. Aumont, C. Baccigalupi, M. Ballardini, A. J. Banday, R. B. Barreiro, N. Bartolo, S. Basak, R. Battye, K. Benabed, J. P. Bernard, M. Bersanelli, P. Bielewicz, J. J. Bock, J. R. Bond, J. Borrill, F. R. Bouchet, F. Boulanger, M. Bucher, C. Burigana, R. C. Butler, E. Calabrese, J. F. Cardoso, J. Carron, A. Challinor, H. C. Chiang, J. Chluba, L. P. L. Colombo, C. Combet, D. Contreras, B. P. Crill, F. Cuttaia, P. de Bernardis, G. de Zotti, J. Delabrouille, J. M. Delouis, E. Di Valentino, J. M. Diego, O. Doré, M. Douspis, A. Ducout, X. Dupac, S. Dusini, G. Efstathiou, F. Elsner, T. A. Enßlin, H. K. Eriksen, Y. Fantaye, M. Farhang, J. Ferguson, R. Fernandez-Cobos, F. Finelli, F. Forastieri, M. Frailis, A. A. Fraisse, E. Franceschi, A. Frolov, S. Galeotta, S. Galli, K. Ganga, R. T. Génova-Santos, M. Gerbino, T. Ghosh, J. González-Nuevo, K. M. Górski, S. Gratton, A. Gruppuso, J. E. Gudmundsson, J. Hamann, W. Handley, F. K. Hansen, D. Herranz, S. R. Hildebrandt, E. Hivon, Z. Huang, A. H. Jaffe, W. C. Jones, A. Karakci, E. Keihänen, R. Keskitalo, K. Kiiveri, J. Kim, T. S. Kisner, L. Knox, N. Krachmalnicoff, M. Kunz, H. Kurki-Suonio, G. Lagache, J. M. Lamarre, A. Lasenby, M. Lattanzi, C. R. Lawrence, M. Le Jeune, P. Lemos, J. Lesgourgues, F. Levrier, A. Lewis, M. Liguori, P. B. Lilje, M. Lilley, V. Lindholm, M. López-Cañiego, P. M. Lubin, Y. Z. Ma, J. F. Macías-Pérez, G. Maggio, D. Maino, N. Mandolesi, A. Mangilli, A. Marcos-Caballero, M. Maris, P. G. Martin, M. Martinelli, E. Martínez-González, S. Matarrese, N. Mauri, J. D. McEwen, P. R. Meinhold, A. Melchiorri, A. Mennella, M. Migliaccio, M. Millea, S. Mitra, M. A. Miville-Deschênes, D. Molinari, L. Montier, G. Morgante, A. Moss, P. Natoli, H. U. Nørgaard-Nielsen, L. Pagano, D. Paoletti, B. Partridge, G. Patanchon, H. V. Peiris, F. Perrotta, V. Pettorino, F. Piacentini, L. Polastri, G. Polenta, J. L. Puget, J. P. Rachen, M. Reinecke, M. Remazeilles, A. Renzi, G. Rocha, C. Rosset, G. Roudier, J. A. Rubiño-Martín, B. Ruiz-Granados, L. Salvati, M. Sandri, M. Savelainen, D. Scott, E. P. S. Shellard, C. Sirignano, G. Sirri, L. D. Spencer, R. Sunyaev, A. S. Suur-Uski, J. A. Tauber, D. Tavagnacco, M. Tenti, L. Toffolatti, M. Tomasi, T. Trombetti, L. Valenziano, J. Valiviita, B. Van Tent, L. Vibert, P. Vielva, F. Villa, N. Vittorio, B. D. Wandelt, I. K. Wehus, M. White, S. D. M. White, A. Zacchei, and A. Zonca, Planck 2018 results. VI. Cosmological parameters, *arXiv e-prints*, [arXiv:1807.06209](https://arxiv.org/abs/1807.06209) (2018), [arXiv:1807.06209 \[astro-ph.CO\]](https://arxiv.org/abs/1807.06209).
- [95] LIGO Scientific Collaboration, *Advanced ligo anticipated sensitivity curves* (2009).
- [96] B. P. Abbott, R. Abbott, T. D. Abbott, M. R. Abernathy, F. Acernese, K. Ackley, C. Adams, T. Adams, P. Addesso, R. X. Adhikari, and et al., Tests of General Relativity with GW150914, *Physical Review Letters* **116**, 221101 (2016), [arXiv:1602.03841 \[gr-qc\]](https://arxiv.org/abs/1602.03841).
- [97] P. Jaiakson, A. Chatrabhuti, O. Evnin, and L. Lehner, Black hole merger estimates in Einstein-Maxwell and Einstein-Maxwell-dilaton gravity, *Phys. Rev. D* **96**, 044031 (2017), [arXiv:1706.06519 \[gr-qc\]](https://arxiv.org/abs/1706.06519).
- [98] J. W. Moffat, Black holes in modified gravity (MOG), *European Physical Journal C* **75**, 175 (2015), [arXiv:1412.5424 \[gr-qc\]](https://arxiv.org/abs/1412.5424).
- [99] V. Varma, S. E. Field, M. A. Scheel, J. Blackman, L. E. Kidder, and H. P. Pfeiffer, Surrogate model of hybridized numerical relativity binary black hole waveforms, *Phys. Rev. D* **99**, 064045 (2019), [arXiv:1812.07865 \[gr-qc\]](https://arxiv.org/abs/1812.07865).

- [100] H. P. Pfeiffer, D. A. Brown, L. E. Kidder, L. Lindblom, G. Lovelace, and M. A. Scheel, Reducing orbital eccentricity in binary black hole simulations, *Classical and Quantum Gravity* **24**, S59 (2007), [arXiv:gr-qc/0702106 \[gr-qc\]](#).
- [101] A. Tsokaros, M. Ruiz, V. Paschalidis, S. L. Shapiro, and K. Uryū, Effect of spin on the inspiral of binary neutron stars, *Phys. Rev. D* **100**, 024061 (2019), [arXiv:1906.00011 \[gr-qc\]](#).
- [102] J. Thornburg, Finding apparent horizons in numerical relativity, *Phys. Rev. D* **54**, 4899 (1996), [arXiv:gr-qc/9508014](#).
- [103] J. Thornburg, A Fast Apparent-Horizon Finder for 3-Dimensional Cartesian Grids in Numerical Relativity, *Class. Quantum Grav.* **21**, 743 (2004), [arXiv:gr-qc/0306056](#).
- [104] A. Ashtekar, C. Beetle, O. Dreyer, S. Fairhurst, B. Krishnan, J. Lewandowski, and J. Wiśniewski, Generic Isolated Horizons and Their Applications, *Phys. Rev. Lett.* **85**, 3564 (2000), [gr-qc/0006006](#).
- [105] A. Ashtekar and B. Krishnan, Isolated and Dynamical Horizons and Their Applications, *Living Reviews in Relativity* **7**, 10 (2004), [gr-qc/0407042](#).
- [106] O. Dreyer, B. Krishnan, D. Shoemaker, and E. Schnetter, Introduction to isolated horizons in numerical relativity, *Phys. Rev. D* **67**, 024018 (2003), [arXiv:gr-qc/0206008](#).
- [107] M. Alcubierre, B. Brügmann, P. Diener, M. Koppitz, D. Pollney, E. Seidel, and R. Takahashi, Gauge conditions for long term numerical black hole evolutions without excision, *Phys. Rev. D* **67**, 084023 (2003), [arXiv:gr-qc/0206072](#).
- [108] J. R. van Meter, J. G. Baker, M. Koppitz, and D.-I. Choi, How to move a black hole without excision: Gauge conditions for the numerical evolution of a moving puncture, *Phys. Rev. D* **73**, 124011 (2006), [gr-qc/0605030](#).
- [109] I. Hinder *et al.*, Error-analysis and comparison to analytical models of numerical waveforms produced by the NRAR Collaboration, *Class. Quant. Grav.* **31**, 025012 (2014), [arXiv:1307.5307 \[gr-qc\]](#).
- [110] H. Kreiss and J. Olinger, *Methods for the Approximate Solution of Time Dependent Problems*, Global Atmospheric Research Programme (GARP): GARP Publication Series, Vol. 10 (GARP Publication, 1973).
- [111] S. R. Brandt and E. Seidel, Evolution of distorted rotating black holes. II. Dynamics and analysis, *Phys. Rev. D* **52**, 870 (1995), [gr-qc/9412073](#).
- [112] R. J. Gleiser, C. O. Nicasio, R. H. Price, and J. Pullin, Evolving the Bowen-York initial data for spinning black holes, *Phys. Rev. D* **57**, 3401 (1998), [gr-qc/9710096](#).
- [113] I. W. Harry and S. Fairhurst, Targeted coherent search for gravitational waves from compact binary coalescences, *Phys. Rev. D* **83**, 084002 (2011), [arXiv:1012.4939 \[gr-qc\]](#).
- [114] L.-V. Collaboration, *Data release for event gw150914* (2016).
- [115] M. Ruiz, M. Alcubierre, D. Núñez, and R. Takahashi, Multiple expansions for energy and momenta carried by gravitational waves, *General Relativity and Gravitation* **40**, 1705 (2008), [arXiv:0707.4654 \[gr-qc\]](#).
- [116] A. Ashtekar and B. Bonga, On the ambiguity in the notion of transverse traceless modes of gravitational waves, *General Relativity and Gravitation* **49**, 122 (2017), [arXiv:1707.09914 \[gr-qc\]](#).
- [117] Y. Zlochower, M. Ponce, and C. O. Lousto, Accuracy issues for numerical waveforms, *Phys. Rev. D* **86**, 104056 (2012), [arXiv:1208.5494 \[gr-qc\]](#).
- [118] Z. B. Etienne, J. G. Baker, V. Paschalidis, B. J. Kelly, and S. L. Shapiro, Improved Moving Puncture Gauge Conditions for Compact Binary Evolutions, *Phys. Rev. D* **90**, 064032 (2014), [arXiv:1404.6523 \[astro-ph.HE\]](#).
- [119] E. A. Huerta, P. Kumar, S. T. McWilliams, R. O'Shaughnessy, and N. Yunes, Accurate and efficient waveforms for compact binaries on eccentric orbits, *Phys. Rev. D* **90**, 084016 (2014), [arXiv:1408.3406 \[gr-qc\]](#).
- [120] A. Nitz, I. Harry, D. Brown, C. M. Biwer, J. Willis, T. D. Canton, C. Capano, L. Pekowsky, T. Dent, A. R. Williamson, M. Cabero, S. De, G. Davies, D. Macleod, B. Machenschalk, P. Kumar, S. Reyes, T. Massinger, F. Pannarale, M. Tápai, dfinstad, S. Fairhurst, S. Khan, A. Nielsen, shasvath, S. Kumar, idorrington92, L. Singer, H. Gabbard, and B. U. V. Gadre, *gwastro/pycbc: Pycbc release v1.14.2* (2019).
- [121] C. M. Biwer, C. D. Capano, S. De, M. Cabero, D. A. Brown, A. H. Nitz, and V. Raymond, PyCBC inference: A python-based parameter estimation toolkit for compact binary coalescence signals, *Publications of the Astronomical Society of the Pacific* **131**, 024503 (2019).
- [122] E. Baird, S. Fairhurst, M. Hannam, and P. Murphy, Degeneracy between mass and spin in black-hole-binary waveforms, *Phys. Rev. D* **87**, 024035 (2013), [arXiv:1211.0546 \[gr-qc\]](#).